

Measurements of Deflection and Residual Stress in Thin Films Utilizing Coherent Light Reflection/Projection Moiré Interferometry

C.A. Sciammarella · A. Boccaccio · L. Lamberti ·
C. Pappalettere · A. Rizzo · M.A. Signore · D. Valerini

Received: 30 July 2012 / Accepted: 26 November 2012 / Published online: 11 January 2013
© Society for Experimental Mechanics 2013

Abstract Thin film technology is an area of great importance in current applications of opto-electronics, electronics, MEMS and computer technology. A critical issue in thin film technology is residual stresses that arise when the coating is deposited onto a substrate. Residual stresses can be very large in magnitude and have detrimental effects on

the role that the thin film must play. To save development time on coating deposition processes it is important to perform accurate residual stresses measurements *in situ* in real time where the deposition is made. A novel optical set up is developed in this study to measure deflections and residual stresses generated in coated specimens that can be applied directly in the reactor utilized in the deposition process. Experimental results are in good agreement with other measurements carried out independently and other data reported in literature for thin films like those tested in the experiments.

C.A. Sciammarella (✉)
Department of Mechanical Engineering, Northern Illinois
University, DeKalb, IL 60115, USA
e-mail: sciammarella@iit.edu

C.A.Sciammarella
e-mail: c.sciammarella@niu.edu

C.A. Sciammarella · A. Boccaccio · L. Lamberti · C. Pappalettere
Dipartimento di Meccanica, Matematica e Management,
Politecnico di Bari,
Bari 70126, Italy

A. Boccaccio
e-mail: a.boccaccio@poliba.it

L. Lamberti
e-mail: lamberti@poliba.it

C. Pappalettere
e-mail: c.pappalettere@poliba.it

C.A. Sciammarella
Department of Mechanical, Materials and Aerospace Engineering,
Illinois Institute of Technology,
Chicago, IL 60616, USA

A. Rizzo · M.A. Signore · D. Valerini
Italian National Agency for New Technologies, Energy and
Sustainable Economic Development, Mesagne 72100, Italy

A. Rizzo
e-mail: antonella.rizzo@enea.it

M.A. Signore
e-mail: maria.signore@enea.it

D. Valerini
e-mail: daniele.valerini@enea.it

Keywords Residual stresses · Thin films · Reflection moiré · Projection moiré

Introduction

Residual stresses in thin films arise because of the existence of discontinuous interfaces, inhomogeneous thermal history during deposition or subsequent fabrication process, and various imperfections by ion bombardment [1–3]. Residual stresses may affect significantly the mechanical properties and reliability of the thin film as well as the performance of thin-film based devices. In particular, high residual stresses will result in detrimental effects in the performance of thin films.

Experimental techniques for measuring residual stresses in thin films and the corresponding equations providing residual stress values are critically revised in [4, 5]. In general, there are two main possible approaches to this problem: (i) lattice strain based methods such as, for example, X-ray diffraction [6], X-ray microdiffraction [7] and neutron diffraction [8]; (ii) physical surface curvature-based methods. However, residual stress values measured by these two methodologies may be quite different because

lattice strain based techniques provide local information while the latter methods provide average data. Lattice-based methods rely on the principle that residual strains and hence residual stresses are caused by the relative displacement between atomic planes: therefore, these techniques measure variations of lattice spacing. Lattice strain methods can be expensive in terms of experimental equipment and can be used only if the films are crystalline.

Determination of residual stress through curvature measurements is easier and less expensive to perform than lattice strain methods and does not introduce constraints on the type of film structure. The average level of residual stress has been computed in many experimental papers using the classical Stoney's equation [9] or variations of this equation (see, for example, [10–12] and the references cited in these papers) which is however valid when the coating is much thinner than the substrate and a number of additional restrictions are satisfied [9–12]. Nano-indentation is the most recent approach and is a commonly used method to measure residual stresses in thin films. It is done by observing how the force-indentation curve changes with respect to a stress free surface (see, for example, the discussion presented in [1, 13] and the references cited in these two articles).

Among curvature measurement methods, non-contact optical techniques are preferable in view of their high sensitivity and because they do not alter the specimen surface. Classical interferometry (i.e., Newton's rings) [14], shearing interferometry [15] or moiré techniques [16–19] can be used to measure curvature of surfaces. Reflection moiré allows measuring the slope of a reflective surface and, through differentiation of the fringe pattern in the frequency space, the curvature of the surface. Projection moiré measures the height of a surface with respect to a reference plane. A system of lines is projected onto the specimen surface and modulated by the curved specimen. The topography of the surface can be obtained from the phase difference generated by the modulation of the grating lines due to the surface curvature. From displacements, derivatives can be computed by differentiation and, from derivatives, surface curvatures can be determined.

This work presents a practical solution of performing measurements of thin plate curvatures *in situ* for diffusing and highly reflecting surfaces. For highly reflecting surfaces, a reflection moiré interferometry set up is developed. The optical set up measures displacements rather than slopes as it is usually done in reflection moiré [17, 19].

The new optical set up developed in this paper is first tested in laboratory measurements of residual stress of a diamond-like-carbon (DLC) thin film, deposited on a quartz substrate via Plasma Enhanced Chemical Vapor Deposition (PECVD). The value of the residual stress developed in the film is derived from the average curvature of the DLC specimen determined via reflection moiré measurements.

Moiré results are in good agreement with experimental values provided by other well established measurement techniques such as Newton's rings and coordinate measuring (CMM) tactile devices. Furthermore, the stress value measured with moiré is consistent with data reported in literature.

The new reflection/projection moiré set up is then implemented *in situ* by designing a special optical circuit. The layout of the optical circuit must satisfy the geometric constraints deriving by the general layout of the deposition system. Measurements carried out for a 1,050 nm thick zirconium nitride film deposited on a 300 μm silicon substrate provide values of residual stress that fall in the range indicated in literature.

The main purpose of the paper is to present the developed optical methodology to measure residual stresses in thin films and the adaptation of this technology to perform measurements *in situ*. The paper is structured as follows: after this introduction, we summarize the basic equations describing the distribution of residual stress generated in the thin film by the deposition process. The third section describes the process of formation of interference fringes and reviews the equations required to compute displacements from reflection moiré patterns. The reflection/projection moiré set up developed in this research is described in detail in the fourth section. Results of moiré measurements carried out on DLC specimens are presented in the fifth section together with Newton's ring and CMM measurements. The sixth section describes the *in situ* implementation of the moiré set up in a vacuum deposition chamber. The main findings of the study are summarized in the last section of the article.

Stress Analysis of the Thin Film

In the Plasma Enhanced Chemical Vapor Deposition (PECVD) process for thin films, an electric discharge generates film precursors, such as neutral radicals and ions, by electron-impact decomposition. Significant residual stresses can develop in the coated specimen because the atoms passing from the gas phase to the substrate during the adsorption process do not reach their correct position in the reticular structure finally formed. As is reported by Davis [2] and Lacerda et al. [3], compressive stresses arise when a growing film is bombarded by atoms or ions with energies of tens or hundreds of eV by a process of "atomic peening". Energetic ions cause atoms to be incorporated into spaces in the growing film which are smaller than the atomic volume of the inserted atoms. This effect causes the expansion of the film outwards with respect to the substrate. The film is constrained by the plate that is bounded to. The effect of the adhesion to the plate is equivalent to apply a

compressive normal force to the film to shorten it to the smaller dimensions of the upper fiber of the plate. If the film is very thin compared to the substratum the stress resultant force of the film, the thickness of the film multiplied by the stress in the film, produces a stress resultant that is assumed to be applied at the upper face of the plate. This force produces a bending moment with respect of the middle fiber of the plate and also a normal stress resultant that equilibrates the stress resultant of the film.

In the general case, the applied coating generates bending stresses and normal stresses. The sign of the stresses depends on the expansion or contraction of the coating with respect to the plate. In Fig. 1, one element of a plate coated with a film is represented for the case that the film tends to expand but it is contracted by the contact with the plate. For the stress analysis of the film-plate system an additional hypothesis is made when films are very thin and their Young's modulus is smaller than that of the substratum. The strains caused by the normal stress resultants are neglected and only the effect of bending is considered. In such a case, following Kirchhoff's plate theory [20], the second derivatives of the deflections define the state of strain and stress on the substrate (Fig. 1) as:

$$\begin{cases} \sigma_{xx} = -\frac{E_s z}{1-\nu_s^2} \left(\frac{\partial^2 w}{\partial x^2} + \nu \frac{\partial^2 w}{\partial y^2} \right) \\ \sigma_{yy} = -\frac{E_s z}{1-\nu_s^2} \left(\frac{\partial^2 w}{\partial y^2} + \nu \frac{\partial^2 w}{\partial x^2} \right) \\ \tau_{xy} = -\frac{E_s z}{1+\nu_s} \cdot \frac{\partial^2 w}{\partial x \partial y} \end{cases} \quad (1)$$

where: $w(x,y)$ is the out-of-plane displacement experienced by the middle plane of the substrate; z is the distance from the middle plane measured in the direction of the curvature radius; E_s and ν_s are respectively the Young's modulus and the Poisson ratio of the substrate material. In the coating the effect of the bending stresses is neglected while in the plate the effect of the normal stresses is neglected when compared to the bending stresses, if the coating rigidity is small compared to the rigidity of the plate.

In the case of diffusing surfaces, projection moiré provides the deflections and through successive differentiations yields the curvatures. Two sets of moiré fringes must be recorded for each analyzed specimen one

yielding the derivatives in the X-direction, the second set yielding the derivatives in the Y direction. By differentiating the two fields with respect to X and with respect to Y, it is possible to obtain the four derivatives and from them it is possible to obtain the curvatures of the surface. The derivatives $\frac{\partial^2 w}{\partial x \partial y}$ and $\frac{\partial^2 w}{\partial y \partial x}$ should be equal since $w(x,y)$ is a continuous function twice differentiable. This property should be used to check that the followed process is correct.

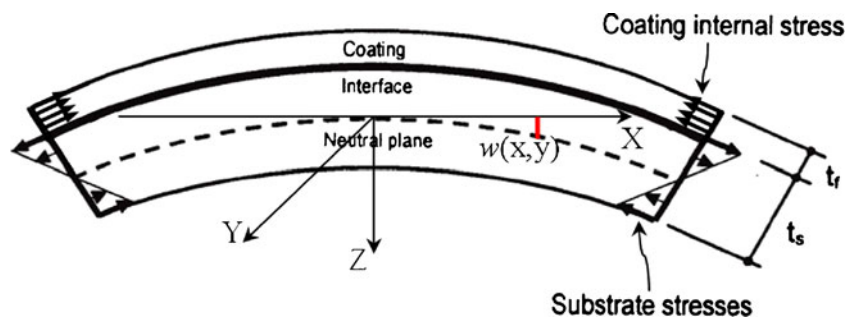
Under the assumption that in-plane stress resultants can be neglected, equation (1) becomes general and can be applied to obtain the stresses in the substrate. If the film is very thin compared to the thickness of the substrate and, assuming that there is a perfect adhesion between the substrate and the film, the strains in the substrate can be computed. By utilizing equilibrium conditions under the same assumptions, if one knows the local values of the film thickness, one can compute the stresses in the thin film.

Under some simplifications of the problem and within the restrictions mentioned in [9–12], the average value of compressive residual stress σ_{film} developed in the thin film can be computed with the modified Stoney's equation:

$$\sigma_{film} = \frac{E_s}{6(1-\nu_s)} \cdot \frac{t_s^2}{t_f} \cdot \left(\frac{1}{R} - \frac{1}{R_o} \right) \quad (2)$$

where R is the principal radius of curvature taken by the specimen after the deposition process at the considered section while R_o is the radius of curvature before deposition. This equation hence assumes that the principal curvatures of the deflected shape of the plate are the same on the film surface. The practical meaning of equation (2) is that the deflected shape is approximately a spherical sector that can be represented by a second order paraboloid. If the deformed shape of the substrate is experimentally determined it is possible to verify the degree of accuracy of this assumption. A brief analysis of the computation of residual stresses is presented in the following because of the utilization of the derived expressions to verify the experimentally measured values of residual stresses after making sure that the corresponding restrictions concerning the applicability of these equations are fulfilled.

Fig. 1 Schematic representation of the stresses developed in the coating and in the substrate. The deposition process generates compressive stresses in the film



There are three forms of moiré that can be applied to measure residual stresses in coated substrates: projection moiré (diffusing surfaces), reflection moiré in the slope measurement mode with one differentiation or projection moiré with two differentiations in the displacement measurement mode. In [19], reflection moiré in the slope mode was utilized to measure residual stresses in 150 mm diameter silicon wafers of thickness 650 μm and coatings of thicknesses of the order of microns. It was found that in most cases twisting curvatures were present although they were one order of magnitude smaller than X and Y-curvatures. For example, in a given typical wafer of the set of specimens studied in [19], the curvatures in the central area of the wafer were $\kappa_x \approx \kappa_y \approx 0.16$ (1/m), that is $R=6.25$ m while the twisting curvature in the same area was $\kappa_x=0.01$ (1/m), that is $R=100$ m. Hence, stress values computed by the Stoney’s equation provide an average of the stresses in the thin film.

For large size substrates, reflection moiré, on the basis of results reported in [19], proved to be a reliable tool to measure residual stresses in thin films deposited on elastic and homogeneous substratum. The question posed in this research now is: Is it possible to apply the same technique utilized in [19] in the case of small size plates? When one measures slopes using reflection moiré a principle similar to finite differentiation (for example, by perturbing spatial coordinate from x to $x+\Delta x$) is applied. Consequently, the coordinate x where the derivative of displacement takes a given value remains indefinite within the range Δx where finite difference is computed. Preliminary testing indicated that the error introduced by following this approach is very significant for a small specimen. Hence, it was decided to utilize reflection moiré to measure deflections for mirror like surfaces. Since in thin film applications surfaces can be diffusing or mirror like, an optical set up that can be applied in either case was developed in this research.

Basic Equation for Reflection Moiré Working in the Deflection Mode

Figure 2 illustrates the process of formation of interference fringes produced by reflection moiré that provides

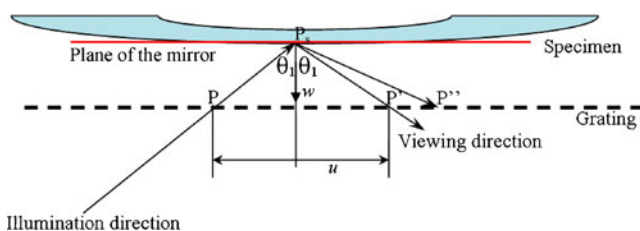


Fig. 2 Measurement of the deflection of a surface with reflection moiré working in the projection moiré modality. Unlike classical reflection moiré, the CCD sensor is focused in the plane of the mirror passing through the point P_s of the specimen surface being considered

the deflection of the surface in place of the surface slope. The moiré pattern is formed by superposing the projected grating and the grating reflected by the object surface. The basic assumption is that the virtual image of the grating as it is reflected by the object surface is being focused in the plane of the mirror (i.e. that corresponding to the reflecting surface, see the schematic in Fig. 2 for the surface point P_s under analysis) and not at some distance from it (i.e. in the plane of the grating, Fig. 2) as it happens instead in the classical reflection moiré used in the slope measurement mode.

The illumination beam is inclined by the angle θ_1 with respect to the normal to the object surface and the point corresponding to P when viewing from a large distance is P' . Because of the surface curvature the point actually corresponding to P is P'' . However, since the distance w between the grating and the specimen surface is small compared to the object dimensions and the distance of the surface to the optical center of the camera, this change of position can be considered negligible: therefore, practically $P' \approx P''$. The change of position of the point P then is:

$$u = 2 w \tan \theta \tag{3}$$

where $\theta = \theta_1 = \theta_2$.

The deflection w can be determined with the classical moiré equation:

$$w = \frac{\phi}{2\pi} \frac{p_j}{2 \tan \theta} \tag{4}$$

where ϕ is the phase of the moiré pattern.

Equation (4) is similar to the equation of shadow moiré except for the factor 2 that comes from the reflection effect. In the above equation, p_j is the pitch of the projected grating. If one utilizes the actual pitch of the grating p_o and recalls the relationship $p_j = p_o/\cos\theta$, equation (4) can be rewritten as:

$$w = \frac{\phi}{2\pi} \frac{p_o}{2 \sin \theta} \tag{5}$$

Consequently, the distribution of light intensity $I(x,y)$ recorded by the sensor at each pixel (x,y) of the image can be expressed as:

$$I(x,y) = I_o(x,y) + I_1(x,y) \times \cos \left[\left(\frac{2\pi}{p_o} \cdot 2 \sin \theta \cdot w(x,y) \right) + \phi_c(x,y) \right] \tag{6}$$

where: $I_o(x,y)$ is the background intensity; $I_1(x,y)$ is the amplitude of the first harmonic, $\phi_c(x,y)$ is the phase modulation term. The phase term $(2\pi/p_o) \cdot 2 \sin \theta \cdot w(x,y)$ corresponding to moiré fringes is equivalent to the phase $(2\pi/p_j) \cdot u(x,y)$ describing the local variations of the projected pitch p_j related to the displacement $u(x,y)$. The intensity

distribution $I(x,y)$ corresponds to the deflection of the plate with respect to the reference plane, not to the surface slope as it would be in the case of classical reflection moiré. Since a carrier is present, not only the value of the deflections can be determined but also their sign.

Experimental Set Up and Reflection Moiré Model in the Deflection Mode

In this study, a reflection moiré set up was developed in order to precisely measure the deflection produced by the deposition process and consequently derive the value of residual stress in the film. The reflection moiré set up is utilized in the deflection measurement mode: therefore, displacement values rather than surface slopes are determined. Figure 3 presents the schematic of the optical set up utilized to measure the out-of-plane displacement field w of the film.

The optical set up is basically comprised of two principal systems: the projection system (PS) and the acquisition system (AS). The optical axis of the projection system is inclined with respect to the optical axis of the acquisition system by the angle $\theta_1=13^\circ$. The projection system includes the laser source L, the polarizer P, the microscope pinhole system PH, the first lens L_1 , the grating G, the second lens L_2 , the iris IR and the third lens L_3 . The acquisition system includes a CCD camera equipped with a long working distance objective.

The images acquired in the experiments were processed with the Holo Moiré Strain Analyzer™ (HMSA) software developed by Sciammarella and his collaborators [21] and supplied by General Stress Optics Inc. (Chicago (IL), USA). The HMSA package includes a very detailed library of state-of-the-art fringe processing tools based on Fourier analysis (Fast Fourier Transform, filtering, carrier modulation, fringe extension, edge detection, masking, removal of discontinuities, etc.). The information on specimen curvature required in the determination of the residual stress field developed in the coating can directly be obtained by applying derivative filters in the frequency space. The theoretical foundation and mathematical steps of the fringe processing operations

performed by the HMSA software are explained in detail in the textbook [17] and in many references cited therein.

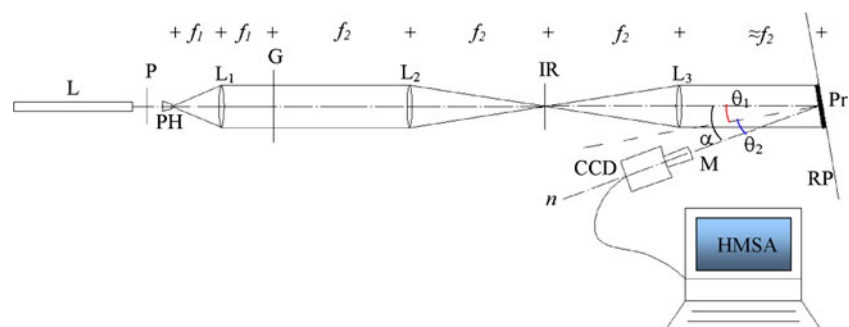
The coherent and polarized light beam generated by the 35 mW He-Ne laser goes through the polarizer P which reduces its intensity. The 40X magnification microscope expands the laser beam. The pinhole system (the nominal diameter of this aperture is $10\ \mu\text{m}$) allows for the removal of noise effects caused by parasitic diffraction phenomena that may occur in the beam expansion process. The exit pupil of the pinhole system is located in the focal plane of the first lens L_1 (focal distance f_1 of 200 mm) hence, the wave front that comes out from lens L_1 is planar. The collimated beam goes through a Ronchi Ruling grating G containing 500 lines/in (this corresponds to have a nominal pitch $p_o=50.8\ \mu\text{m}$) and is focused by the second lens L_2 . In the focal plane of this lens (i.e. at the focal distance $f_2=300\ \text{mm}$ from lens L_2), is observed the Fourier transform of the light wave front diffracted by the grating G. In this focal plane, the iris IR can be opened so to select orders 0 and one of the ± 1 orders to produce a sinusoidal carrier with the projected grating pitch. The light beam coming out from the iris is then collimated by the lens L_3 ($f_2=f_3$). The collimated wave front carrying the filtered spectrum of the grating is projected onto the reference plane that is basically a mirror to which it is attached the specimen SP to be analyzed.

The light wave front that impinges the mirror or the sample is reflected back to the sensor of the CCD camera. However, this does not mean that the optical set up works in the reflection moiré modality. In fact, the sensor is focused right on the surface of the sample and not on the reference plane [22].

An objective with long working distance (denoted as M in the schematic of Fig. 3) was coupled with a CCD camera able to focus planes located at a distance longer than 50 cm. The field of view of the sensor was as large as the DLC specimen under investigation. The recording system includes also an auxiliary lens and a 2X lens to maximize resolution.

Figure 4(a) shows the assembly view of the moiré set up while Fig. 4(b) shows the detail of the reference plane with the specimen attached to it. A high precision frame onto which the reference plane is fixed allowed the reflected

Fig. 3 Schematic of the optical set up used for measuring film residual stresses



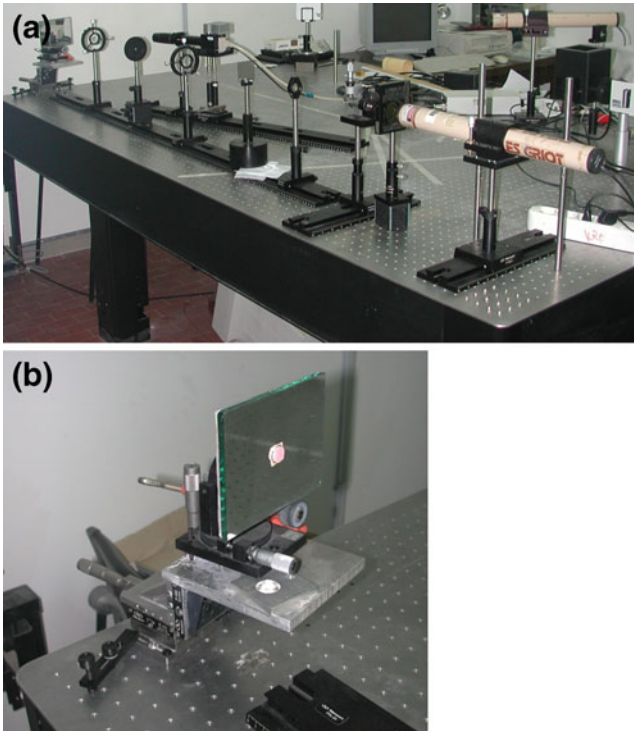


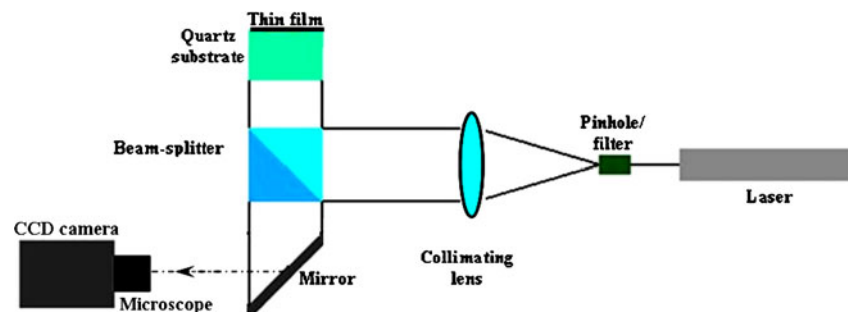
Fig. 4 Moiré set up utilized in the residual stress measurement: (a) 3D assembly view of the optical set up; (b) Detail of the reference plane and DLC specimen

beam to be precisely lined up with the axis of the CCD camera.

Experimental Results: Laboratory Tests on DLC Specimens

The moiré set up described in the previous section was tested in laboratory to determine the residual stress developed in a diamond-like carbon thin film deposited on a quartz substrate. The specimen is circular in shape with a diameter of 1 cm. The nominal thickness of the quartz substrate is 2 mm (i.e. 2,000 μm) while the nominal thickness of the coating is 1 μm (i.e. 1,000 nm). Elastic properties of the quartz substrate were set as follows: $E=94$ GPa and $\nu=0.17$.

Fig. 5 Optical set up used for interferometric measurements with Newton's rings



The angle of illumination $\theta_1=13^\circ$ was measured by analyzing the change in spatial frequency of the projected grating when no specimen is mounted onto the reference mirror. Care was taken to achieve the nominal condition of reflection $\theta=\theta_1=\theta_2$ as accurately as possible. The projected pitch $p_j=p_o/\cos\theta$ is 52.14 μm . The corresponding sensitivity $p_j/(2\tan\theta)$ is 112.9 μm .

Prior to performing the moiré test, the curvature of the DLC specimen was measured by means of the Newton's rings interferometric technique. The experimental set up is schematized in Fig. 5. The image recording system including the CCD camera and the microscope is the same utilized in the case of moiré measurements. On the average, a total number of 33 rings were counted on the specimen surface (see Fig. 6) and fractional orders were neglected. The specimen was properly positioned so to lie in the center of the image field. The total deflection was determined as the product between the average number of interference fringes (i.e. 33) and the measurement sensitivity which is half of the wavelength of the He-Ne laser light ($\lambda=632.8$ nm) used in the experiments. Therefore, it was found $\delta_{\text{DLC}}=33 \times 0.3164 \mu\text{m}=10.44 \mu\text{m}$. The margin of possible differences of the final result is $\pm 0.3164 \mu\text{m}$, that is one fringe order since the deflection was obtained by fringe counting and the error was estimated to be one order.

The deflection of the DLC specimen was also measured with a tactile mechanical device, a Zeiss Contura[®] G2 coordinate measuring machine (CMM) operating under the Calypso software. The specified accuracy of the CMM machine is 1 μm . The deflection was measured along 10 profiles passing through the center of the circular specimen surface. The average value of deflection, 10.8 μm with a standard deviation of $\pm 0.3 \mu\text{m}$, measured by CMM hence is in excellent agreement with interferometric measurements.

Since the maximum deflection to be measured was about 1/10 of the sensitivity of the moiré set up, the nominal grating pitch of 50.8 μm was rated good for carrying out the moiré experiments. Figure 7(a) and (b) show respectively the phase maps obtained for the specimen surface and the reference plane. The corresponding phase difference is shown in Fig. 7(c). As expected, the phase difference corresponds to less than one order. It is very difficult to achieve

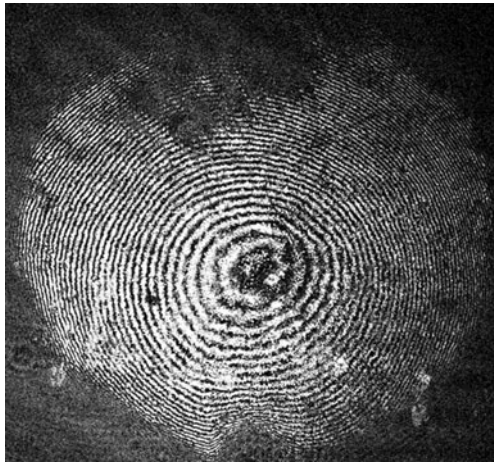
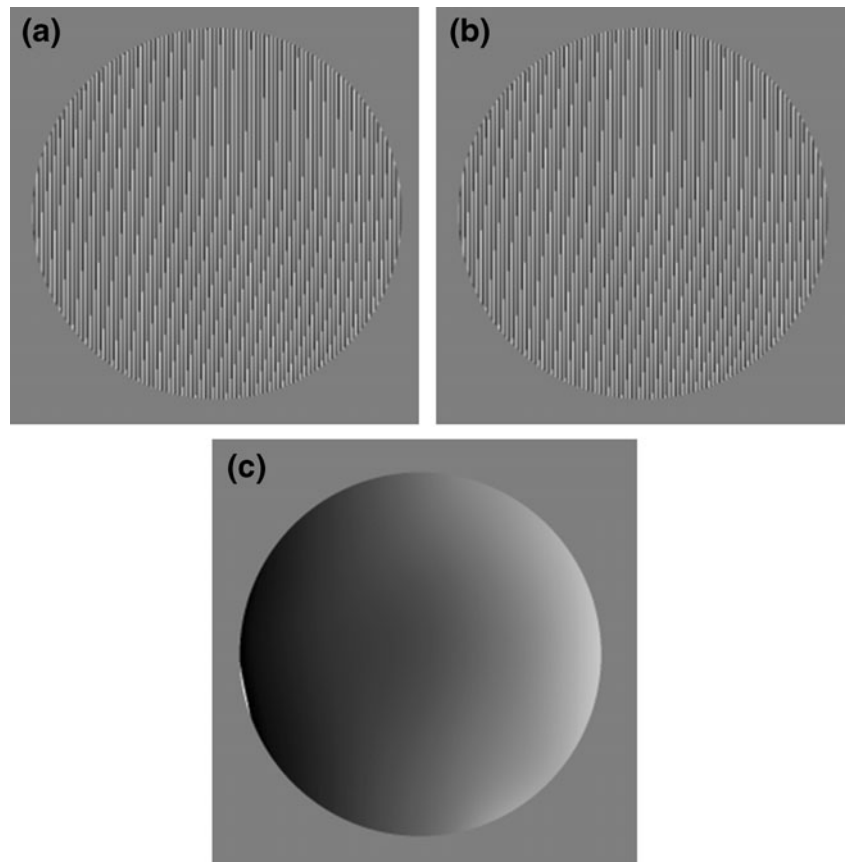


Fig. 6 Newton's rings pattern recorded for the DLC specimen

the condition of parallelism between the specimen surface and the reference plane. Due to this fact, the deflected surface is referred to an inclined plane. This effect is corrected with a MATLAB routine and the displacement map finally obtained is shown in Fig. 8: the 3-D plot of the specimen's deflection is shown in Fig. 8(a) while the corresponding contour lines, that appear very regular, are plotted in Fig. 8(b). It should be noted that Fig. 8 presents the absolute values of measured deflection. In the DLC

Fig. 7 (a) Phase of the DLC specimen surface; (b) Phase of the reference plane; (c) Phase difference



experiment, the back face of the quartz plate was observed since this face is highly reflecting when compared to the film surface. The coated face expands and thus it becomes convex while the observed surface was concave.

The resulting deflection measured by the moiré set up is $10.45 \mu\text{m}$ value obtained by fitting experimental orders of the deflection to a second order parabolic function (see Fig. 9) which is almost identical to the value of the deflection measured by means of the Newton's rings interferometric technique and very close to the values measured by the tactile CMM device. In particular, the difference between the CMM and the moiré method is 3.35 %. It should be noted that some distortions were observed in the shape of the Newton's rings but no correction routines were implemented for that pattern as the goal of the interferometric measurement was just to have information on the order of the magnitude of the expected deflection.

Since the three measurements performed with moiré, Newton's rings and the CMM device were totally independent and based on different physical principles, it can be concluded that the value of deflection measured with the moiré set up presented in this paper is reliable and within the bounds of experimental results variations.

The data file of surface point coordinates given in output by the HMSA software was further processed by means of a MATLAB routine in order to determine the value of the

radius of curvature of the film after deposition. The routine twice differentiated the deflection data at the point of maximum deflection and gave a radius of curvature of 1.598 m.

In order to determine the average residual stress in the film, the modified Stoney's equation (2) was chosen in view of the arguments presented in this paper and considering the final purpose of the system, to measure residual stresses *in situ*. The application of the modified Stoney's equation (2) requires the knowledge of the initial radius of curvature of the substratum. To obtain a reliable value for R_0 , substrata that have the same geometric dimensions and went through the same fabrication process as the DLC substratum were analyzed: the measured value of R_0 was 1.729 m.

In order to verify the assumed hypothesis that the shape of the deformed membrane can be represented by a paraboloid, a cross-section of Fig. 8(a) was plotted and a quadratic function was fitted to the deflected shape (see Fig. 9). Figure 9 shows that the assumed behavior of the deformation of the substrate is satisfied on the average and provides a value of the curvature, the second derivative of the fitted second order polynomial, $\kappa=0.6052$ (1/m). This value differs from the value obtained by the MATLAB routine by 3.4 %, hence there is a very good agreement. Taking the curvature value given by the plot in Fig. 9 as a more representative value than the numerical value of

Fig. 8 (a) Deflection of the coated plate measured in the case of the DLC specimen; (b) Contour lines of the deflection map shown in Fig. 8(a). Absolute values of deflection are represented in the plots

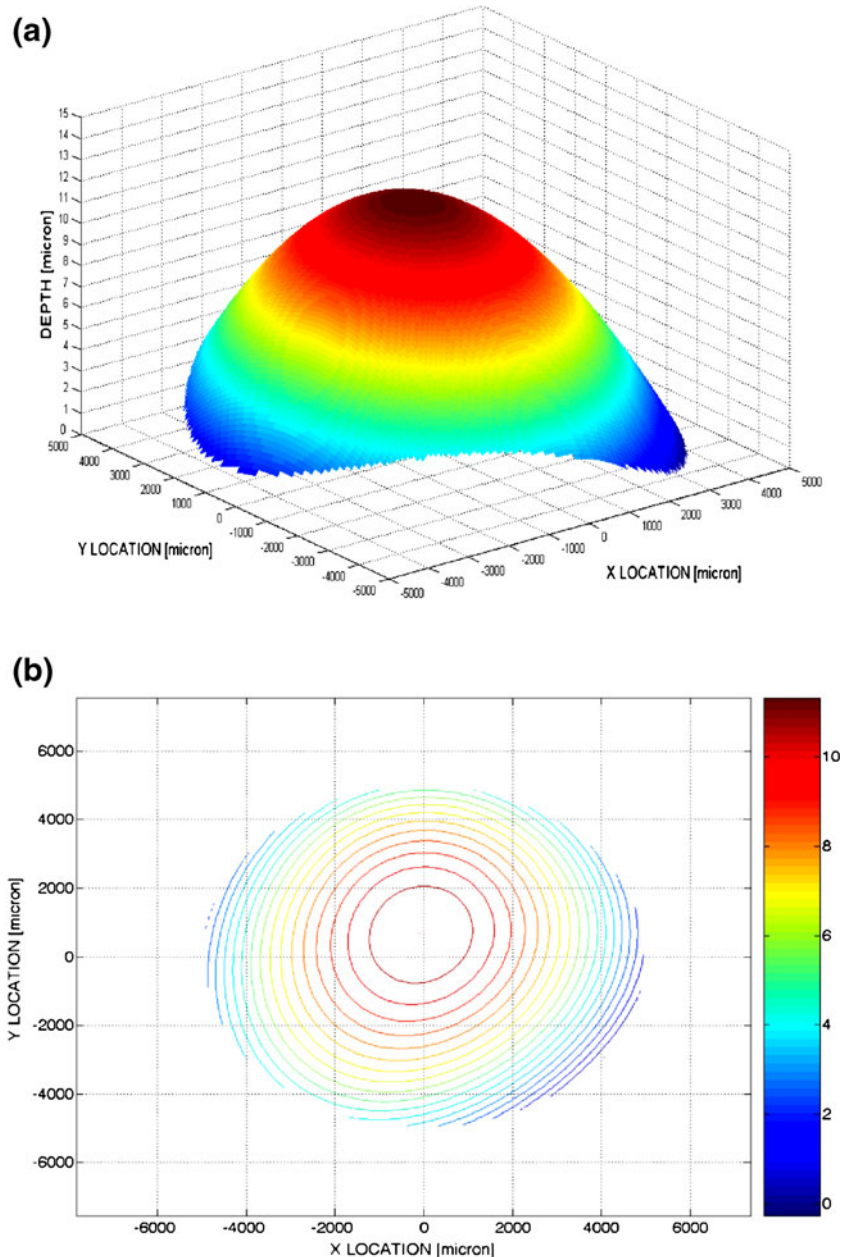
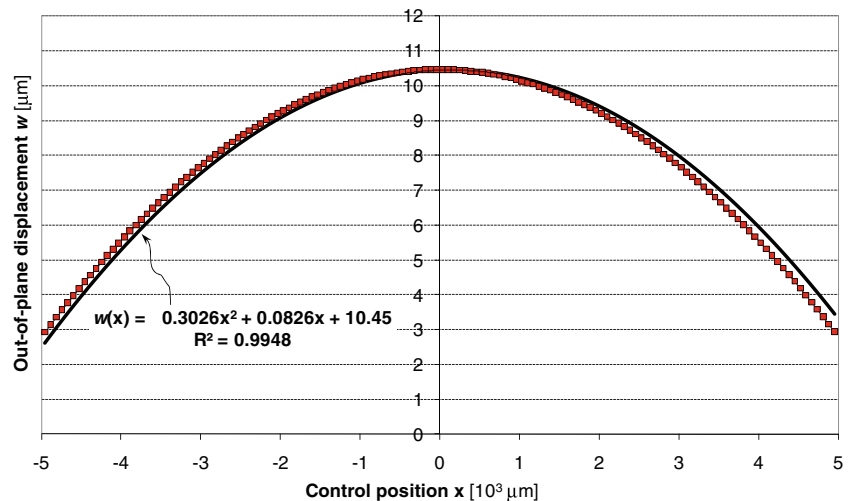


Fig. 9 Plot of the cross-section of Fig. 8 and polynomial equation providing the shape of the cross-section



the second derivative obtained by finite differences and replacing it and the initial curvature value into the modified Stoney's formula (2) yields,

$$\begin{aligned}\sigma_{\text{film}} &= -\frac{94 \cdot 10^9 \text{ Pa}}{6 \cdot (1 - 0.17)} \cdot \frac{(2 \cdot 10^{-3})^2 \text{ m}^2}{1 \cdot (10^{-6})\text{m}} \\ &\quad \cdot (0.6052 - 0.5784) \frac{1}{\text{m}} \\ &= -2.02 \text{ GPa}\end{aligned}$$

where the minus sign indicates that the thin film has compressive residual stress. This value is realistic and consistent with data reported in literature [23, 24].

The obtained result indicates that the reflection moiré method used in the deflection measurement mode can be utilized to determine an average value of the residual stresses on a small circular plate. A very simple procedure, the fitting of the measured deflections with a paraboloid surface, provides the value of the curvature that must be given in input in the Stoney's equation. It becomes feasible to implement a real time procedure to get information about the deposition process *in situ* and in real time.

In Situ Implementation of the Reflection/Projection Moiré Set Up

The encouraging results obtained in the DLC laboratory tests in terms of agreement between moiré experimental data, other measurements performed independently and literature data led us to adapt the novel reflection/projection moiré set up to a real vacuum deposition chamber. The goal was to measure *in situ* the level of residual stress developed in the thin film during the deposition process. For that purpose, a special optical circuit was designed. Figure 10 (a) shows the vacuum chamber for thin film deposition instrumented with the moiré optical set up. The whole

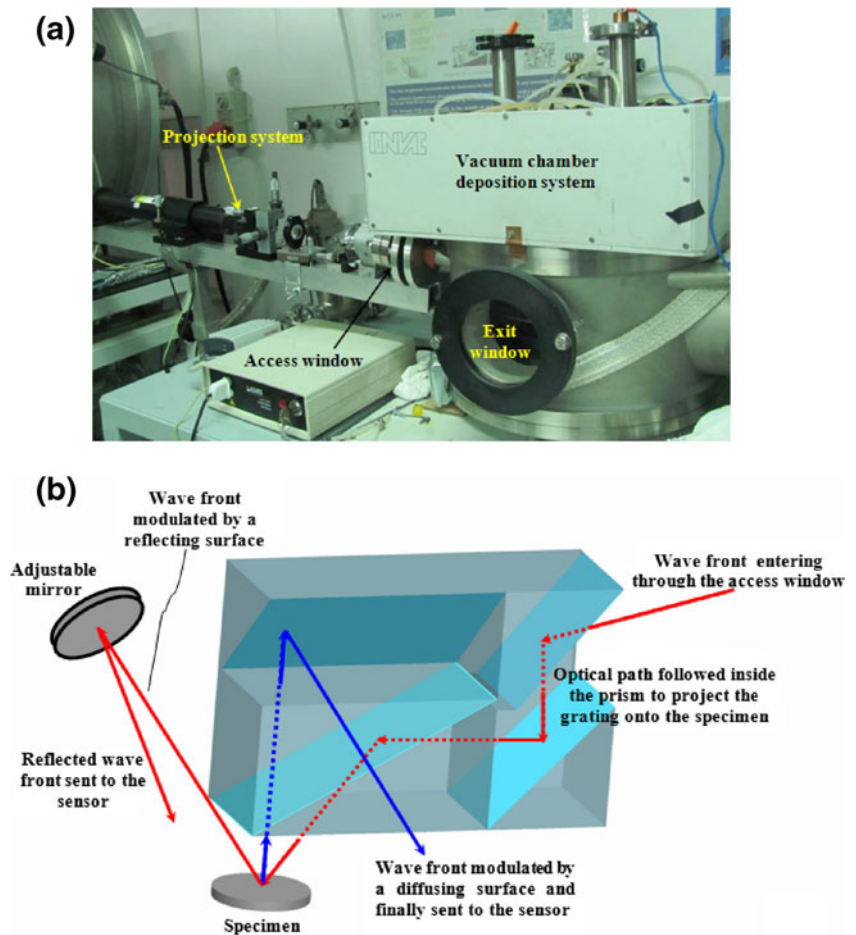
system is now physically located in the Thin Films Laboratory of the Italian National Agency for New Technologies, Energy and Sustainable Economic Development (ENEA), Mesagne (Italy).

The original laboratory set up described in “[Experimental set up and Reflection Moiré Model in the Deflection Mode](#)” was modified in order to fit in the general layout of the deposition chamber. The chamber has two large windows of given dimensions and fixed position. One window was used as the access window for carrying the illuminating wave front through which the grating is projected. The other window was utilized as the exit window to record moiré patterns. The projection system was mounted onto a prismatic arm rigidly supported and lined up with the access window (see Fig. 10(a)).

The grating was projected onto the specimen submitted to deposition by a composite prism system located near the exit window. Figure 10(b) shows a 3D schematic of this prism system. The laser beam carrying the image of the projected grating passes through the access window of the vacuum deposition chamber, then experiences three successive reflections and is finally directed onto the specimen. The optical set up allows performing measurements on both reflecting and diffusing objects. In the case of reflecting surfaces, the image is reflected on the adjustable mirror to align the beam with the camera sensor. In the case of a diffusing surface, the direction of observation is normal to the specimen. The modulated wave front is hence reflected by the prism back to the exit window and then imaged by the CCD sensor.

Preliminary tests were conducted to optimize the quality of the images acquired by the sensor. The brightness and contrast of the pattern of lines recorded in the experiments depend on the reflection/diffusion properties of the film deposited onto the substrate. Diffraction figures eventually created by some residual curvature of the access and exit windows through which the laser beam passes can be removed by properly selecting harmonics in the filtering operations. In order to simplify measurements and avoid damage

Fig. 10 (a) Assembly view of the vacuum chamber deposition system equipped with the reflection/projection moiré system (the optical prism and the adjustable mirror are fixed to the supporting frame); (b) 3D schematic of the optical circuit that allows the grating to be projected onto the specimen and the light wave front modulated by the specimen to be sent to the sensor



of the prism surface, film deposition must be done at the longest distance from the exit window. The luminescence produced by the deposition process did not affect the intensity distribution of the modulated grating recorded by the CCD sensor either because deposition occurred far away from the prism and the colour of light emitted in the deposition process (light violet) did not overlap with the CCD camera sensitivity spectrum.

The residual stress produced by a zirconium nitride (ZrN) film of thickness 1,050 nm deposited on a silicon substrate of thickness 300 μm was measured. Elastic properties of the substrate were set as follows: $E=150$ GPa and $\nu=0.17$. The spatial frequency of the grating used in the experiments was 317.5 μm (i.e. 80 lines/in). As the prism was designed so that the angle made by the direction of illumination with the normal to the specimen surface is 32.3°, the corresponding value of sensitivity $p_f/(2\tan\theta)$ adopted in the *in situ* measurements on the reflecting object surface is 299.6 μm .

Since no significant variation in the spatial frequency of the lines projected onto the sample before the beginning of the deposition process could be detected by the moiré set up, it was concluded that the initial curvature of the substrate must be negligible. After the deposition process, the spatial frequency of the lines modulated by the object increased in

correspondence of the sample edges thus indicating that the out-of-plane displacement field generated by the deposition process has a maximum in the central region of the specimen. By processing the moiré pattern it was found a total deflection of 9.7 μm which corresponds to a curvature radius of 1.45 m. By substituting these values in the Stoney's formula (2) with $1/R_0=0$ (i.e. no initial curvature), it was possible to determine a residual stress of 1.78 GPa. This result is consistent with similar data reported in literature [25]. In this case, the reflectivity of the coating produced good quality patterns.

Concluding Remarks

The research work presented in the paper is the first step towards the application of moiré to routine *in situ* measurements of residual stresses generated in thin films during the deposition process. For that purpose, a reflection moiré optical set up working in the projection moiré modality was developed and tested in laboratory on diamond-like carbon thin film specimens. The deflection measured with moiré was found to be consistent with Newton's rings interferometric measurements and CMM tactile device measurements carried out independently. The

applicability of the Stoney's equation to determine the residual stresses in the film by fitting the deformed shape of the substratum to a parabolic surface was verified by the observed results that confirm residual stresses measurements on large size substrata utilizing reflection moiré in the slope measurement mode [19].

The encouraging results of laboratory tests then led us to implement the novel moiré set up described in the article in a real vacuum deposition chamber located in the Thin Films Laboratory of the Italian National Agency for New Technologies, Energy and Sustainable Economic Development (ENEA), Mesagne (Italy). The optical circuit was adapted to the layout of the deposition chamber. The experimental set up can treat both reflecting and diffusing objects. *In situ* measurements were successfully carried out in the case of ZrN thin films deposited on a silicon substrate finding stress values consistent with data recently published in literature. The results presented in this paper fully demonstrate the feasibility of use of reflection/projection moiré for real time measurements of residual stress developed in the thin film deposition process. The process can be completely automated by introducing electronic circuitry that does the fringe processing in real time.

References

- Lee YH, Takashima K, Kwon D (2004) Micromechanical analysis on residual stress-induced nanoindentation depth shifts in DLC films. *Scr Mater* 50(9):1193–1198
- Davis CA (1993) A simple model for the formation of compressive stress in thin films by ion bombardment. *Thin Solid Films* 226(1):30–34
- Lacerda RG, Marques FC, Freire FL (1999) The subimplantation model for diamond-like carbon films deposited by methane gas decomposition. *Diam Relat Mater* 8(2–5):495–499
- Zhao ZB, Hershberger J, Yalisove SM, Bilello JC (2002) Determination of residual stress in thin films: a comparative study of X-ray topography versus laser curvature method. *Thin Solid Films* 415(1–2):21–31
- Kang KJ, Yao N, He MY, Evans AG (2003) A method of *in situ* measurement of the residual stress in thin films by using the focussed ion beam. *Thin Solid Films* 443(1–2):71–77
- Zheng X, Li J, Zhou Y (2004) X-ray diffraction measurement of residual stress in PZT thin films prepared by pulsed laser deposition. *Acta Mater* 52:3313–3322
- Brown MA, Rosakis AJ, Feng X, Huang Y, Üstündag E (2007) Thin film/substrate systems featuring arbitrary film thickness and misfit strain distributions. Part II: experimental validation of the non-local stress/curvature relations. *Int J Solids Struct* 44(6):1755–1767
- Ahmed R, Faisal NH, Paradowska AM, Fitzpatrick ME (2012) Residual strain and fracture response of Al₂O₃ coatings deposited via APS and HVOF techniques. *J Therm Spray Tech* 21(1):23–40
- Stoney GG (1909) The tension of metallic films deposited by electrolysis. *Proc R Soc Lond Ser A* 82:172–175
- Von Preissig FJ (1989) Applicability of the classical curvature-stress relation for thin films on plate substrates. *J Appl Phys* 66(9):4262–4268
- Feng X, Huang Y, Rosakis AJ (2007) On the Stoney formula for a thin film/substrate system with nonuniform substrate thickness. *J Appl Mech Trans ASME* 74(6):1276–1281
- Ngo D, Feng X, Huang Y, Rosakis AJ, Brown MA (2007) Thin film/substrate systems featuring arbitrary film thickness and misfit strain distributions. Part I: analysis for obtaining film stress from non-local curvature information. *Int J Solids Struct* 44(6):1745–1754
- Lepienski CM, Pharr GM, Park YJ, Watkins TR, Misra A, Zhang X (2004) Factors limiting the measurement of residual stresses in thin films by nanoindentation. *Thin Solid Films* 447–448:251–257
- Born M, Wolf E (2002) Principles of optics, 7th edn. Cambridge University Press, Cambridge
- Dong X, Feng X, Hwang KC, Ma S, Ma Q (2011) Full-field measurement of nonuniform stresses of thin films at high temperature. *Opt Express* 19(14):13201–13208
- Sciammarella CA (2003) Overview of optical techniques that measure displacements: Murray Lecture. *Exp Mech* 43(1):1–19
- Sciammarella CA, Sciammarella FM (2012) Experimental mechanics of solids: theory, techniques, instrumentation and applications. Wiley-Blackwell, New York
- Sciammarella CA, Trentadue B, Sciammarella FM (2000) Measurement of bending stresses in shells of arbitrary shape using the reflection moiré method. *Exp Mech* 40(3):282–288
- Sciammarella CA, Combet O (1995) Interferometric reflection moiré. In: RJ Pryputniewicz, GM Brown, WP Juptner (eds) Interferometry VII, applications. Proceedings of SPIE 2545: 72–85
- Timoshenko S (1940) Theory of plates and shells. McGraw-Hill, New York
- General Stress Optics Inc. (2008) Holo-Moiré strain analyzer software HoloStrain™, version 2.0. Chicago (IL), USA. <http://www.stressoptics.com>
- Ebbeni J (1966) Etude du phénomène de moirure par réflexion d'un réseau plan sur une surface gauchie et de son application en analyse des contraintes et des déformations. *VDI Experimentelle Spannung Analyse Berichte* 102:75–81
- Tomasella E, Meunier C, Mikhailov S (2001) a-C:H thin films deposited by radio-frequency plasma: influence of gas composition on structure, optical properties and stress levels. *Surf Coat Technol* 141(2–3):286–296
- Kulikovskiy V, Vorliceck V, Bohac P, Kurdyumov A, Deyneka A, Jastrabik L (2003) Thermal stability of microhardness and internal stress of hard a-C films with predominantly sp² bonds. *Diam Relat Mater* 12(8):1378–1384
- Meng QN, Wen M, Qu CQ, Hu CQ, Zheng WT (2011) Preferred orientation, phase transition and hardness for sputtered zirconium nitride films grown at different substrate biases. *Surf Coat Technol* 205(8–9):2865–2870